THREE-DIMENSIONAL COMPUTATIONAL FLUID DYNAMICS MODELING OF TiO_2/R134a NANOREFRIGERANT

by

Kamil ARSLAN*

Mechanical Engineering Department, Karabuk University, Karabuk, Turkey

Original scientific paper
DOI:10.2298/TSCI140425002A

In this study, numerical investigations were carried out for R134a based TiO_2 nanorefrigerants. Forced laminar flow and heat transfer of nanorefrigerants in a horizontal smooth circular cross-sectioned duct were investigated under steady--state condition. The nanorefrigerants consist of TiO_2 nanoparticles suspended in R134a as a base fluid with four nanoparticle volume fractions of 0.0, 0.8, 2.0, and 4.0%. Numerical studies were performed under laminar flow conditions where Reynolds numbers range from $8 \cdot 10^2$ to $2.2 \cdot 10^3$. Flow is flowing in the duct with hydrodynamically and thermally developing (simultaneously developing flow) condition. The uniform surface heat flux with uniform peripheral wall heat flux (H2) boundary condition was applied on the duct wall. Commercial CFD software, ANSYS Fluent 14.5, was used to carry out the numerical study. Effect of nanoparticle volume fraction on the average convective heat transfer coefficient and average Darcy friction factor were analyzed. It is obtained in this study that increasing nanoparticle volume fraction of nanorefrigerant increases the convective heat transfer in the duct, however, increasing nanoparticle volume fraction does not influence the pressure drop in the duct. The velocity and temperature distribution in the duct for different Reynolds numbers and nanoparticle volume fractions were presented.

Key words: *TiO_2/R134a nanorefrigerant, nanoparticle volume fraction, forced convection, friction factor, heat transfer coefficient, laminar flow*

Introduction

Enhancement of heat transfer performance on the fluid used for convective heat transfer apparatus is one of the most studied topics recently. Adding solid nanoparticles, which have high thermal conductivity, in the fluids, is one of the techniques used for enhancement of convective heat transfer of the fluids. As a result of studies conducted recently within 10-50 nm-sized solid nanoparticles in suspension shows that convective heat transfer of the fluids enhances surprisingly. Nanofluids are produced by dispersion of nanometer sized (1-100 nm) solid nanoparticles having high thermal conductivity (such as Cu, TiO_2, Al_2O_3, *etc.*) in a base fluid (such as water, oil, glycol, *etc.*). Nanofluids are used in engineering devices to enhance the heat transfer capabilities. The applications of nanofluids are very wide. Nanofluids are used numerous applications, such as tribology, chemistry, environmental areas, surfactants and coating, pharmaceutical, and medical applications. They are also used in super conducting magnets,

* Author's e-mail: kamilarslan@karabuk.edu.tr

microprocessors, jacket water cooling in vehicles, and fuel cells [1]. In the previous works, nanofluids have been investigated by various authors with experimental and numerical studies. Kamyar [1] reviews and summarizes the numerical studies performed in fluid flow of nanofluids including conventional numerical methods. Moraveji and Ardehali [2] and Moraveji *et al*. [3-5] carried out numerical investigation for nanofluids. They investigated the thermal performance of the various nanofluids with different nanoparticle concentrations. The Al_2O_3, TiO_2, and SiC nanoparticles were used dispersed in the water and non-Newtonian fluid (Xanthan). They obtained that heat transfer coefficient increased with increasing nanoparticle concentration and Reynolds number. Hussein *et al*. [6, 7] investigated numerically the effect of cross-sectional area of tubes on turbulent TiO_2-water nanofluid flow. Circular, elliptical and flat tube cross-sections were used in the numerical investigations. Moraveji and Hejazian [8] used Fe_3O_4-water magnetic nanofluid for their numerical investigations. Effect of nanoparticle concentration of magnetic nanofluid on heat transfer and friction factor were examined. Lelea and Nisulescu [9] carried out numerical investigation for fluid flow of Al_2O_3-water nanofluid through the micro tube. The viscous dissipation effect with different volume concentration rates was considered in the study. Hojjat *et al*. [10] examined experimentally laminar flow convective heat transfer of non-Newtonian nanofluids in a circular tube with constant wall temperature. The carboxymethyl cellulose solution was used for base fluid and Al_2O_3, TiO_2, and CuO were used for nanoparticles. It was obtained that the convective heat transfer enhancement is more significant when both the Peclet number and the nanoparticle concentration were increased. Mohammed *et al*. [11] investigated numerically the effect of using Al_2O_3-water nanofluid on heat transfer and fluid flow in rectangular shaped micro-channel heat sink. It was seen that presence of nanoparticles enhanced the cooling of micro-channel under extreme heat flux conditions. Also, there were slight increase in the pressure drop in the micro-channel is found compared with the pure water cooling. Bianco *et al*. [12] numerically investigated developing laminar forced convection flow of Al_2O_3-water nanofluid in a circular tube with uniform heat flux at the wall. Single- and two-phase model (discrete nanoparticles model) was employed with either constant or temperature dependent properties. It was obtained that the maximum difference in the average heat transfer coefficient between single- and two-phase models results was about 11%. Chein and Chuang [13] carried out experimental study for fluid flow of different volume concentration CuO-water nanofluid in micro-channel heat sink. It was found that nanofluid absorbed more energy than base fluid when the flow rate was low. For high flow rates, the heat transfer dominated by the flow rate and nanoparticles did not contribute to the extra heat absorption. Also, it was seen that slightly increase in pressure drop due to the presence of nanoparticles. Heris *et al*. [14] examined experimentally Cu-water nanofluid flow through a circular tube. Laminar flow condition and constant wall temperature boundary condition were used in the study. The Nusselt number of nanofluids for different nanoparticle concentrations and various Peclet numbers were obtained. Also, the rheological properties of the nanofluid for different volume fractions of nanoparticles were measured and compared with theoretical models. It was found that convective heat transfer was enhanced by increasing nanoparticle concentrations and Peclet number. Li and Xuan [15] built an experimental system to investigate convective heat transfer and flow characteristics of the Cu-water nanofluid in circular cross-sectioned duct. Study was performed under both laminar and turbulent flow conditions. It was seen that the convective heat transfer coefficient was increased about 60% for the nanofluid 2.0 vol% Cu nanoparticles compared with the base fluid at the same Reynolds number. New convective heat transfer correlations for laminar and turbulent flow conditions were established. Yang *et al*. [16] measured convective heat transfer coefficients of several graphite nanofluids under laminar

flow condition in a horizontal tube heat exchanger. The results were compared with the correlations obtained from literature. Kaya [17] numerically analyzed the Al_2O_3-water nanofluid flow in a square duct with uniform heat flux for different volume fractions. The study was performed under turbulent flow condition. It was obtained that for a given Reynolds number, increasing the volumetric concentration of nanoparticles did not have a significant effect on the velocity contours. Also, at a constant dimensionless temperature, increasing the nanoparticle volume concentration changes the dimensionless temperature profile. Salman *et al*. [18] summarized numerous researches on the fluid flow and heat transfer behavior of different types of micro tubes and micro-channel at different orientations and nanofluids. They gave detailed summary for preparation, properties, and behavior of nanofluids. Also, influence of several parameters such as the geometrical specifications, boundary conditions, and type of fluids on the fluid flow was presented in this study. Kuppusamy *et al*. [19] performed numerical investigation for fluid flow and heat transfer characteristics of various types of nanofluids in a trapezoidal grooved micro-channel heat sink. The influence of the width, depth, and pitch of the groove on the thermal performance of the trapezoidal grooved micro-channel heat sink was examined. The effects of nanoparticle types, volume fraction, and nanoparticle diameter on the fluid flow and heat transfer in trapezoidal grooved micro-channel heat sink were also studied. It is obtained that Al_2O_3-water had the highest thermal performance with 0.04 volume fraction and 25 nm nanoparticle diameter. Kherbeet *et al*. [20] examined the effect of step height on the flow and heat transfer characteristics of laminar mixed convective SiO_2-ethylene glycol nanofluid flow over a 3-D horizontal microscale backward-facing step. The immersed SiO_2 nanoparticle in ethylene glycol was considered as 25 nm nanoparticle diameter with 0.04 volume fraction. It was observed that the Nusselt number and skin friction coefficient increased with increasing the step height. Mohammed and Narrein [21] investigated the effects of using different geometrical parameters with the combination of nanofluid on heat transfer and fluid flow characteristics in a helically coiled tube heat exchanger numerically. The CuO-water nanofluid was used for this study. The CuO nanoparticle with a diameter of 25 nm dispersed in water with a nanoparticle concentration of 4% was considered as a working fluid for this study. It was presented that the helix radius and inner tube diameter affected the performance of the helically coiled tube heat exchanger. Tokit *et al*. [22] analyzed the laminar fluid flow and heat transfer performance in the interrupted micro-channel heat sink using nanofluids. The Al_2O_3, CuO, and SiO_2 nanoparticles of nanoparticle diameter in the range of, 30 nm to 60 nm immersed in pure water with volume fraction in the range of 1% to 4% were used as nanofluid in this study. The effects of the transport properties, nanofluid type, nanoparticle volume fraction, and nanoparticle diameter on the thermal performance of interrupted micro-channel heat sink were investigated in detail. The highest and lowest thermal performance in the heat sink was obtained for Al_2O_3-water nanofluid and SiO_2-water nanofluid, respectively. The Nusselt number increased with the increasing of nanoparticle volume fraction and with the decreasing of nanoparticle diameter.

If the base fluid of the nanofluid is the refrigerant, it is named as nanorefrigerant, which is prepared by mixing nanoparticles with refrigerant. Nanorefrigerants have lots of advantages: Firstly, nanoparticles enhance the solubility between the lubricant and the refrigerant. The thermal conductivity of the refrigerants increases with mixing nanoparticles. Nanoparticles dispersed in refrigerant decrease the pressure lost [23]. The detailed review investigation on nanoparticles suspended with refrigerants and lubricating oils in refrigeration systems was carried out by Saidur *et al*. [24]. Jiang *et al*. [25] measured the thermal conductivities of CNT/R113 nanorefrigerants. It was obtained that thermal conductivity of CNT/R113 nanorefrigerants increased compared with pure R113. Peng *et al*. [26] carried out experimental study for

CuO-R113 nanorefrigerants fluid flow in horizontal circular cross-sectioned duct. They investigated the convective heat transfer coefficients of CuO-R113 nanorefrigerants flow. It was found that nanorefrigerants had larger convective heat transfer coefficients than pure refrigerants. Jwo *et al*. [27] performed experimental study for domestic refrigerators using Al_2O_3-mineral oil. The experimental results showed that power consumption was reduced with using Al_2O_3-mineral oil as a refrigerant.

It is obtained from literature review that the heat transfer characteristics of base fluids increase with adding nanoparticles. This paper is to investigate the fluid flow of nanorefrigerant in a circular cross-sectioned duct with constant heat flux is applied on the duct wall. The TiO_2 nanoparticle with a diameter of 25 nm dispersed in R134a with different nanoparticle volume fractions (0.8, 2.0, and 4.0%) was used as the working fluid in this study. The present study concerns 3-D flow under hydrodynamically and thermally developing flow conditions. The study was carried out under laminar flow region. The momentum, continuity, and energy equations for 3-D flow in the hydrodynamic and thermal entrance region of circular cross-sectioned duct were solved using finite volume based commercial software ANSYS Fluent 14.5. Practical engineering correlations for the average heat transfer coefficient and average Darcy friction factor were determined. This study will provide the basic data for the application of the nanorefrigerants in the refrigeration systems.

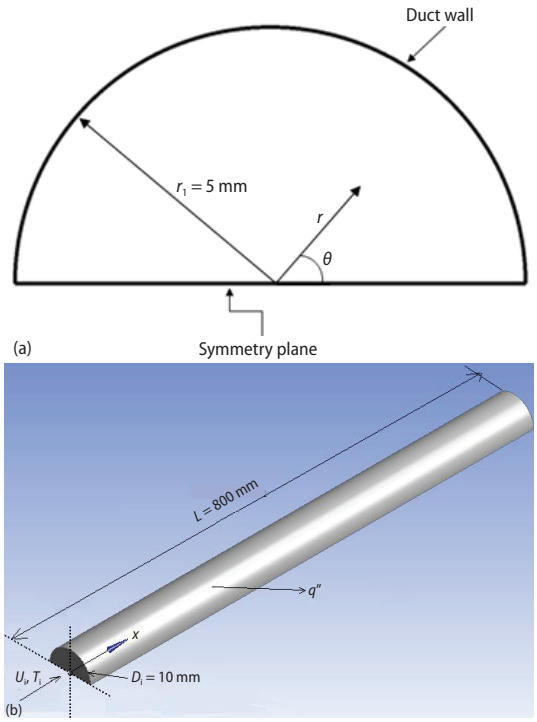

Figure 1. (a) Cross-section of the duct; (b) computational domain of the duct with boundary conditions

Theoretical description

Laminar forced flow and heat transfer of TiO_2-R134a nanorefrigerant in a circular cross-sectioned duct was investigated numerically. A schematic diagram depicting the cross-section and computational domain of the duct along with the co-ordinate system and dimensions of the flow geometry were presented in figs. 1(a) and 1(b). Since the flow field is symmetric, only one half of the channel has been considered in the numerical calculations for reducing the computational time. The diameter and the length of the circular cross-sectioned duct are 10 mm and 800 mm, respectively.

The 3-D continuity, momentum and energy equations were used to describe the flow and heat transfer in the computational domains. The 3-D incompressible flow with negligible buoyancy effects and viscous dissipation was regarded as laminar and steady. Since the diameter of nanoparticles less than 100 nm, single phase approach was considered in this study [3]. The fluid phase was considered as continuous.

Governing equations of continuity, momentum, and energy are given as [12]:

– continuity equation

$$\mathrm{div}(\rho\vec{\mathrm{V}}) = 0 \tag{1}$$

– momentum equation

$$\mathrm{div}(\rho\vec{\mathrm{V}}\vec{\mathrm{V}}) = -\mathrm{grad}\,P + \nabla(\mu\nabla\vec{\mathrm{V}}) \tag{2}$$

– energy equation

$$\mathrm{div}(\rho c_p \vec{\mathrm{V}}T) = \mathrm{div}(k\,\mathrm{grad}\,T) \tag{3}$$

The thermal and physical properties of nanorefrigerant were determined from eqs. (4)-(12) [19, 28]:

$$\rho_{\mathrm{nf}} = (1-\phi)\rho_{\mathrm{f}} + \phi\rho_{\mathrm{p}} \tag{4}$$

$$c_{p,\mathrm{nf}} = \frac{\phi(\rho_{\mathrm{p}}.c_{p,\mathrm{p}}) + (\rho_{\mathrm{f}}.c_{p,\mathrm{f}})(1-\phi)}{\rho_{\mathrm{nf}}} \tag{5}$$

$$\mu_{\mathrm{nf}} = \mu_{\mathrm{nf,static}} + \mu_{\mathrm{nf,Brownian}}$$
$$\mu_{\mathrm{nf,static}} = \frac{\mu_{\mathrm{f}}}{(1-\phi)^{2.5}} \tag{6}$$

$$\mu_{\mathrm{nf,Brownian}} = 5\cdot 10^4 \beta\phi\rho_{\mathrm{f}}\sqrt{\frac{\kappa T}{\rho_{\mathrm{p}} d_{\mathrm{p}}}} f(T,\phi) \tag{7}$$

$$k_{\mathrm{nf}} = k_{\mathrm{nf,static}} + k_{\mathrm{nf,Brownian}} \tag{8}$$

$$k_{\mathrm{nf,static}} = k_{\mathrm{f}}\left[\frac{k_{\mathrm{p}} + k_{\mathrm{f}}(n-1) - \phi(n-1)(k_{\mathrm{f}} - k_{\mathrm{p}})}{k_{\mathrm{p}} + k_{\mathrm{f}}(n-1) + \phi(k_{\mathrm{f}} - k_{\mathrm{p}})}\right] \tag{9}$$

$$k_{\mathrm{nf,Brownian}} = 5\cdot 10^4 \beta\phi\rho_{\mathrm{f}} c_{p,\mathrm{f}}\sqrt{\frac{\kappa T}{\rho_{\mathrm{p}} d_{\mathrm{p}}}} f(T,\phi) \tag{10}$$

In eq. (9), n is the empirical shape factor given by $3/\psi$, and ψ is the nanoparticle sphericity, defined as surface area of a sphere (with the same volume as the given nanoparticle) to the surface area of the nanoparticle. For spherical nanoparticle the value of n is 3 [28]. The nanoparticle diameter of TiO_2 is d_{p}=25 nm, β – the fraction of the liquid volume which travels with a nanoparticle and κ – the Boltzmann constant and defined as:

$$\kappa = 1.3807\cdot 10^{-23}\ \ [\mathrm{JK}^{-1}] \tag{11}$$

The $f(T,\phi)$ can be obtained with:

$$f(T,\phi) = (2.817\cdot 10^{-2}\phi + 3.917\cdot 10^{-3})\left(\frac{T}{T_o}\right) + (-3.0669\cdot 10^{-2}\phi - 3.91123\cdot 10^{-3}) \tag{12}$$

The thermo-physical properties of R134a and TiO_2 are presented in tab. 1 [29].

The continuity, momentum, and energy equations were solved by using ANSYS Fluent 14.5. The fluid enters the duct with uniform velocity and temperature profile. No slip boundary conditions were employed on the duct walls. A uniform heat flux with uniform peripheral wall heat flux was applied on the surface of the duct. Symmetry boundary condition was employed on the

Table 1. The thermo-physical properties of R134a and TiO_2

Thermo-physical properties	R134a	TiO_2
Density, ρ [kgm^{-3}]	1199.7	4157
Specific heat, c_p [Jkg^{-1}K^{-1}]	1432	710
Thermal conductivity, k [Wm^{-1}K^{-1}]	$80.3\cdot10^{-3}$	8.4
Dynamic viscosity, μ [Nsm^{-2}]	$19.05\cdot10^{-5}$	–

symmetry plane. At the outlet of the duct, pressure outlet boundary condition of ANSYS Fluent 14.5 was used.

The objectives of the data reduction are to calculate the average Nusselt number and Reynolds number along with average Darcy friction factor:

$$\mathrm{Re} = \frac{UD_\mathrm{h}}{\nu} \tag{13}$$

$$\mathrm{Nu} = \frac{hD_\mathrm{h}}{k} \tag{14}$$

$$f = \frac{\Delta P\left(\frac{D_\mathrm{h}}{L}\right)}{\rho\left(\frac{U^2}{2}\right)} \tag{15}$$

Average convective heat transfer coefficient of the flow in duct is obtained by Cengel and Ghajar [30]:

$$h = \frac{q''}{T_\mathrm{w} - T_\mathrm{b}} \tag{16}$$

In this study, a general purpose finite volume based commercial CFD software package ANSYS Fluent 14.5 has been used to carry out the numerical study. The software provides mesh flexibility by structured and unstructured meshes.

Computations were performed under laminar flow conditions. The energy equation was solved neglecting radiation effects. In the present study, tetrahedron cells were created with a fine mesh near the duct walls. Boundary layer mesh was used near the surfaces of the duct for obtaining fine mesh distribution. A non-uniform grid distribution was employed in the plane perpendicular to the main flow direction as shown in fig. 2. Close to each wall, the number of grid points or control volumes was increased to enhance the resolution and accuracy.

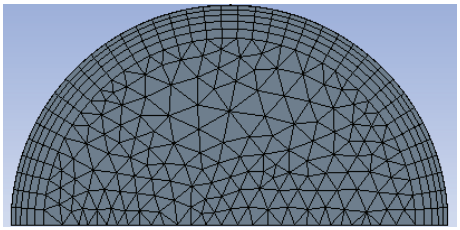

Figure 2. Mesh distribution of the duct

Steady segregated solver was used with second order upwind scheme for convective terms in the mass, momentum, and energy equations. For pressure discretization, the standard scheme has been employed while the SIMPLE algorithm [31] has been used for pressure-velocity coupling discretization.

The grid independence study was performed by refining the grid size until the variation in both average Nusselt number and average Darcy friction factor were less than 0.73% and 0.38%, respectively [32]. To assure the accuracy of the results presented, a grid independence study was conducted using ten different grid sizes changing from $2.6\cdot10^4$ to $3.4\cdot10^5$ to study the effects of grid size. It was observed that a further refinement of grids from $2.5\cdot10^5$ to $3.4\cdot10^5$ did not have a significant effect on the results in terms of average Nusselt number and average Darcy friction factor as seen in fig. 3.

Based on this observation, grid size of $2.5 \cdot 10^5$ points was used for all of the calculations. No convergence problems were observed. Same procedure was used for other nanoparticle volume fractions and optimum grid size was obtained for different calculations. To obtain convergence, each equation for mass, momentum, and energy equations have been iterated until the residual falls below $1 \cdot 10^{-6}$.

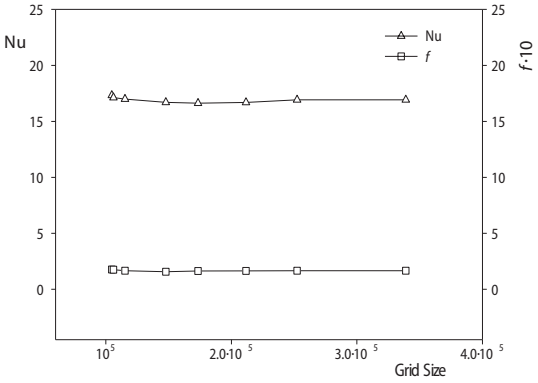

Figure 3. Grid size effect for average Nusselt number and average Darcy friction factor

Results and discussion

In the study reported here, convective heat transfer and fluid friction of TiO_2/R134a nanorefrigerant in a circular cross-sectioned duct under uniform surface heat flux with uniform peripheral wall heat flux was numerically investigated. The investigation was carried out under hydrodynamically and thermally developing laminar flow condition. The results were presented in convective heat transfer coefficient and Darcy friction factor. After the determination of temperature fields in the nanorefrigerant flow in the duct, the average convective heat transfer coefficients were calculated. In addition, average Darcy friction factors were estimated with the determination of pressure drop in the duct. Numerical results obtained under steady-state conditions were presented in fig. 4 through fig. 9. The flow velocity and temperature distributions, the average convective heat transfer coefficients and average Darcy friction factors were presented in this study to highlight the influence of the nanorefrigerant on the thermal performance of duct flow and provide additional useful design data.

Before starting numerical analysis on nanorefrigerants, the reliability and accuracy of numerical measurements were tested by using base fluid R134a. Numerical results were compared with the correlation provided by Sieder and Tate [33] for laminar flow in the thermal entrance region. It is shown in fig. 4 that the results of numerical investigation are harmonious with the Sieder and-Tate correlation [33], which emphasizes on the accuracy and reliability of the numerical results.

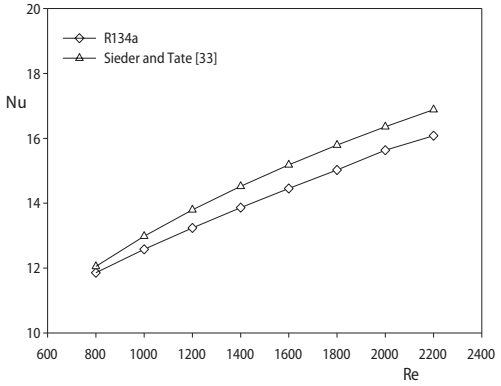

Figure 4. Comparison between the heat transfer results of numerical investigation and Sieder-Tate equation for base fluid R134a

After the validation of the numerical analysis, the effect of the flow condition and nanoparticle volume fraction of nanorefrigerant on the fluid flow and heat transfer in duct flow was examined. Velocity distribution at the outlet of the duct can be shown in fig. 5 for nanoparticle volume fraction of 4.0% and different Reynolds numbers. It is seen in this figure that velocity profile changes with changing Reynolds numbers. The maximum velocity occurs at the center of the duct. The velocity magnitude in the duct decreases towards to the duct wall, however, it increases with increasing Reynolds number.

Figure 6 shows the temperature distribution at the outlet of the duct for nanoparticle volume fraction of 4.0% and different Reynolds numbers. Temperature contours in the duct have different

profiles for different Reynolds numbers. Also, temperature decreases gradually towards to center of the duct from the surface. It can be seen from the figure that minimum temperature occurs at the center of the duct. Also, the temperature magnitude in the duct decreases with increasing fluid velocity.

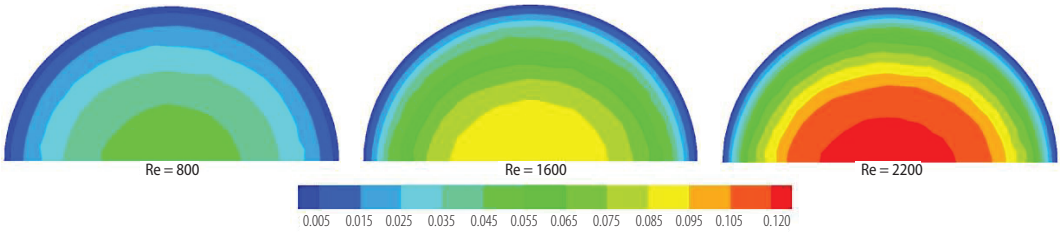

Figure 5. Velocity distributions at the outlet of the duct for different Reynolds numbers
(*for color image see journal web site*)

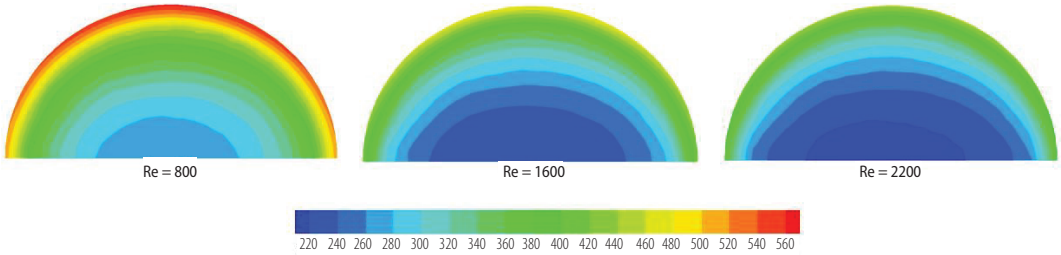

Figure 6. Temperature distributions at the outlet of the duct for different Reynolds numbers
(*for color image see journal web site*)

Velocity and temperature distribution at the outlet of the duct for Re = $2.2 \cdot 10^3$ and different nanoparticle volume fractions were presented in figs. 7 and 8, respectively. It is obtained in the figures that increasing the nanoparticle volume fraction does not have significant effect on the velocity and temperature profiles. While the velocity magnitude decreases towards the duct wall, the temperature magnitude increases.

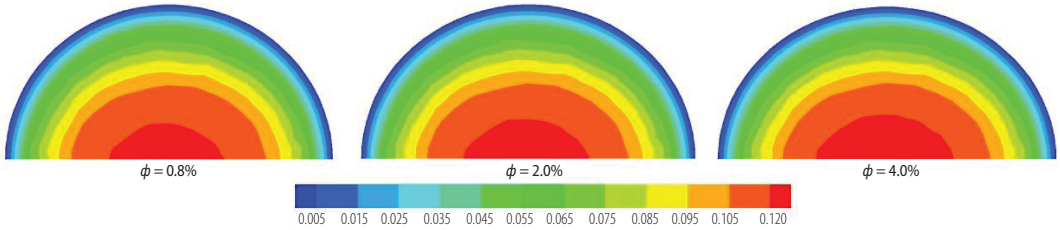

Figure 7. Velocity distributions at the outlet of the duct for different nanoparticle volume fractions
(*for color image see journal web site*)

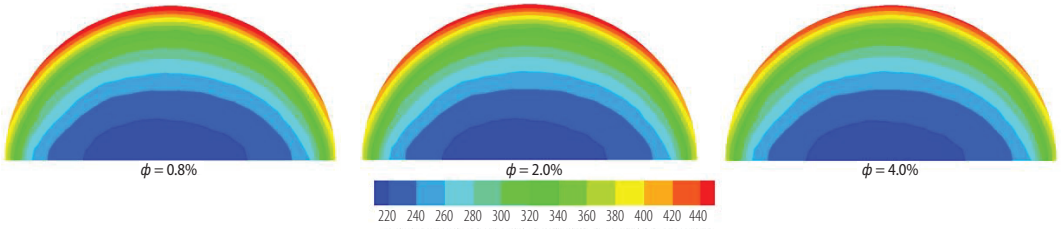

Figure 8. Temperature distributions at the outlet of the duct for different nanoparticle volume fractions
(*for color image see journal web site*)

Equations (17) and (18) show the power law variation of average heat transfer coefficient and average Darcy friction factor with Reynolds number and nanoparticle volume fraction, respectively. These equations have been obtained using least-square method and are valid for $8 \cdot 10^2 < \mathrm{Re} < 2.2 \cdot 10^3$ and $0.8\% < \phi < 4.0\%$.

$$h = 14.38\,\mathrm{Re}^{0.3}\,\phi^{0.05} \tag{17}$$

$$f = \frac{78.35\phi^{0.05}}{\mathrm{Re}^{0.8}} \tag{18}$$

The changing of average heat transfer coefficient and average Darcy friction factor with Reynolds number are presented in figs. 9(a) and 9(b) for different nanoparticle volume fractions, respectively. The results show that increasing Reynolds number increases the average heat transfer coefficient, however, reduces the average Darcy friction factor. Also, it is seen that, average heat transfer coefficient increases with increasing nanoparticle volume fractions. The pure R134a has smaller heat transfer coefficients compared with state of added nanoparticles. On the other hand, the value of average Darcy friction factor is not varied with addition of nanoparticles in R134a. While the nanorefrigerant of nanoparticle volume fraction of 4.0% increases the heat transfer coefficient almost 9.0%, there is no remarkable increase in pressure drop. Therefore, it is obtained that the nanorefrigerant of nanoparticle volume fraction of 4.0% is the significant nanorefrigerant for this study.

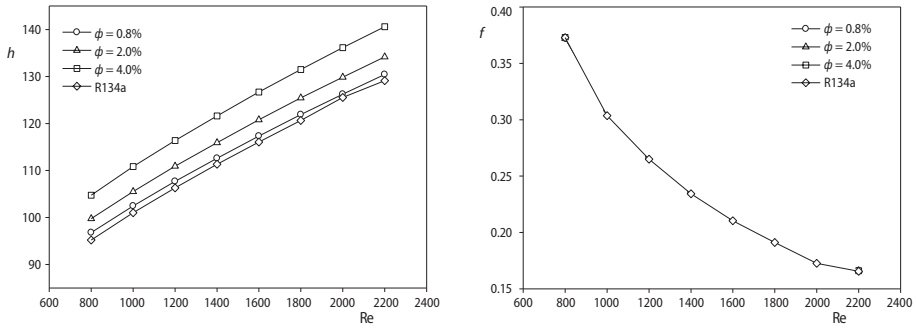

Figure 9. The changing of (a) average heat transfer coefficient, and (b) average Darcy friction factor with Reynolds number for different nanoparticle volume fractions

Conclusions

Heat transfer and fluid friction of R134a based TiO_2 nanorefrigerants for different nanoparticle volume fractions were numerically investigated in this study. The hydrodynamically and thermally developing 3-D steady laminar flow conditions in a horizontal circular cross-sectioned duct were carried out. Reynolds number was changing from $8 \cdot 10^2$ to $2.2 \cdot 10^3$. The results of numerical computations were presented in terms of average heat transfer coefficients and average Darcy friction factors. It is obtained in this study that increasing the Reynolds number increases the average heat transfer coefficients. On the other hand, average Darcy friction factor decreases with increasing Reynolds number. Also, average heat transfer coefficient increases with increasing nanoparticle volume fractions, however, the value of average Darcy friction factor is unchanged with addition of nanoparticles into R134a.

Based on the present 3-D numerical solutions of R134a based TiO_2 nanorefrigerants for different nanoparticle volume fractions of laminar flow in the hydrodynamic and thermal

entrance region, new engineering correlations are presented for the average heat transfer coefficient and average Darcy friction factor. The velocity and temperature distribution for different Reynolds numbers and nanoparticle volume fractions in the duct were presented graphically. It is also obtained from the study that the TiO_2 nanoparticle addition into the R134a increases the convection heat transfer in the duct up to 9.0% compared with the pure R134a.

Acknowledgement

The author would like to thank the Cankiri Karatekin University Research and Development Center, Turkey for financial support of this project (Project no: BAP 2012/24).

Nomenclature

c_p – specific heat, [Jkg^{-1}K^{-1}]
d_p – nanoparticle diameter, [nm]
D_h – hydraulic diameter of the passageway through the considered duct, [m]
f – average Darcy friction factor, [–]
h – average heat transfer coefficient in the duct, [Wm^{-2}K^{-1}]
k – thermal conductivity, [Wm^{-1}K^{-1}]
L – axial length of the duct, [m]
n – empirical shape factor, [–]
Nu – average Nusselt number for the steady-state heat transfer in the duct, [–]
ΔP – pressure drop along the duct, [Pa]
P – pressure, [Pa]
q'' – steady-state rate of convective heat flux, [Wm^{-2}]
Re – hydraulic diameter based Reynolds number, [–]
r_i – inner radius of the duct, [m]
T – fluid temperature, [K]
T_b – mean bulk temperature in the duct, $(=\int_A \rho u T \mathrm{d}A / \int_A \rho u \mathrm{d}A)$, [K]
T_w – surface temperature of the duct, [K]
U_i – inlet nanorefrigerant velocity, [ms^{-1}]
U – mean velocity in the duct, [ms^{-1}]
x, r, θ – cylindrical co-ordinates, [–]
V – axial velocity, [ms^{-1}]

Greek symbols

β – fraction of the liquid volume which travels with a nanoparticle, [–]
κ – Boltzmann constant, [JK^{-1}]
μ – dynamic viscosity, [Nsm^{-2}]
ν – kinematic viscosity, [m^{2}s^{-1}]
ρ – density, [kgm^{-3}]
ψ – nanoparticle sphericity, [–]
ϕ – nanoparticle volume fraction, [–]

Subscript

nf – nanofluid
p – nanoparticle
f – base fluid

References

[1] Kamyar, A., *et al*., Application of Computational Fluid Dynamics (CFD) for Nanofluids, *International Journal of Heat and Mass Transfer*, *55* (2012), 15-16, pp. 4104-4115
[2] Moraveji, M. K., Ardehali, R. M., CFD Modeling (Comparing Single and Two-Phase Approaches) on Thermal Performance of Al_2O_3-water Nanofluid in Mini-Channel Heat Sink, *International Communications in Heat and Mass Transfer, 44* (2013), May, pp. 157-164
[3] Moraveji, M. K., *et al*., Modeling of Convective Heat Transfer of a Nanofluid in the Developing Region of Tube Flow with Computational Fluid Dynamics, *International Communications in Heat and Mass Transfer, 38* (2013), 9, pp. 1291-1295
[4] Moraveji, M. K., *et al*., CFD Investigation of Nanofluid Effects (Cooling Performance and Pressure Drop) in Mini-Channel Heat Sink, *International Communications in Heat and Mass Transfer, 40* (2013), Jan., pp. 58-66
[5] Moraveji, M. K., *et al*., Modeling of Forced Convective Heat Transfer of a Non-Newtonian Nanofluid in the Horizontal Tube under Constant Heat Flux with Computational Fluid Dynamics, *International Communications in Heat and Mass Transfer, 39* (2012), 7, pp. 995-999
[6] Hussein, A. M., *et al*., The Effect of Cross-Sectional Area of Tube on Friction Factor and Heat Transfer Nanofluid Turbulent Flow, *International Communications in Heat and Mass Transfer, 47* (2013), Oct., pp. 49-55

[7] Hussein, A. M., *et al*., Heat Transfer Enhancement with Eliptical Tube under Turbulent Flow TiO_2-Water Nanofluid, *Thermal Science, 20* (2016), 1, pp. 89-97
[8] Moraveji, M. K., Hejazian, M., Modeling of Turbulent Forced Convective Heat Transfer and Friction Factor in a Tube for Fe_3O_4 Magnetic Nanofluid with Computational Fluid Dynamics, *International Communications in Heat and Mass Transfer, 39* (2012), 8, pp. 1293-1296
[9] Lelea, D., Nisulescu, C., The Micro-Tube Heat Transfer and Fluid Flow of Water Based Al_2O_3 Nanofluid with Viscous Dissipation, *International Communications in Heat and Mass Transfer, 38* (2011), 6, pp. 704-710
[10] Hojjat, M., *et al*., Laminar Convective Heat Transfer of Non-Newtonian Nanofluids with Constant Wall Temperature, *Heat and Mass Transfer, 47* (2011), 2, pp. 203-209
[11] Mohammed, H. A., *et al*., Heat Transfer in Rectangular Microchannels Heat Sink Using Nanofluids, *International Communications in Heat and Mass Transfer, 37* (2010), 10, pp. 1496-1503
[12] Bianco, V., *et al*., Numerical Investigation of Nanofluids Forced Convection in Circular Tubes, *Applied Thermal Engineering, 29* (2009), 17-18, pp. 3632-3642
[13] Chein, R., Chuang, J., Experimental Microchannel Heat Sink Performance Studies Using Nanofluids, *International Journal of Thermal Sciences, 46* (2007), 1, pp. 57-66
[14] Heris, S. Z., *et al*., Convective Heat Transfer of a Cu-water Nanofluid Flowing through a Circular Tube, *Experimental Heat Transfer, 22* (2009), 4, pp. 217-227
[15] Li, Q., Xuan, Y., Convective Heat Transfer and Flow Characteristics of Cu-Water Nanofluid, *Science in China (Series E)*, *45* (2002), 4, pp. 408-416
[16] Yang, Y., *et al*., Heat Transfer Properties of Nanoparticle-in-Fluid Dispersions (Nanofluids) in Laminar Flow, *International Journal of Heat and Mass Transfer, 48* (2005), 6, pp. 1107-1116
[17] Kaya, O., Numerical Study of Turbulent Flow and Heat Transfer of Al_2O_3-Water Mixture in a Square Duct with Uniform Heat Flux, *Heat and Mass Transfer, 49* (2013), 11, pp. 1549-1563
[18] Salman, B. H., *et al*., Characteristics of Heat Transfer and Fluid Flow in Microtube and Microchannel Using Conventional Fluids and Nanofluids: A Review, *Renewable and Sustainable Energy Reviews, 28* (2013), Dec., pp. 848-880
[19] Kuppusamya, N. R., *et al*., Numerical Investigation of Trapezoidal Grooved Microchannel Heat Sink Using Nanofluids, *Thermochimica Acta, 573* (2013), Dec., pp. 39-56
[20] Kherbeet, A. Sh., *et al*., The Effect of Step Height of Microscale Backward-Facing Step on Mixed Convection Nanofluid Flow and Heat Transfer Characteristics, *International Journal of Heat and Mass Transfer, 68* (2014), Jan., pp. 554-566
[21] Mohammed, H. A., Narrein, K., Thermal and Hydraulic Characteristics of Nanofluid Flow in a Helically Coiled Tube Heat Exchanger, *International Communications in Heat and Mass Transfer, 39* (2012), 9, pp. 1375-1383
[22] Tokit, E. M., *et al*., Thermal Performance of Optimized Interrupted Microchannel Heat Sink (IMCHS) Using Nanofluids, *International Communications in Heat and Mass Transfer,* 39 (2012), 10, pp. 1595-1604
[23] Bi, S., *et al*., Performance of a Domestic Refrigerator Using TiO_2-R600a Nano-Refrigerant as Working Fluid, *Energy Conversion and Management, 52* (2011), 1, pp. 733-737
[24] Saidur, R., *et al*., A Review on the Performance of Nanoparticles Suspended with Refrigerants and Lubricating Oils in Refrigeration Systems, *Renewable and Sustainable Energy Reviews, 15* (2011), 1, pp. 310-323
[25] Jiang, W. T., *et al*., Measurement and Model on Thermal Conductivities of Carbon Nanotube Nanorefrigerants, *International Journal of Thermal Science, 48* (2009), 6, pp. 1108-1115
[26] Peng, H., *et al*., Heat Transfer Characteristics of Refrigerant-Based Nanofluid Flow Boiling inside a Horizontal Smooth Tube, *International Journal of Refrigeration, 32* (2009), 6, pp. 1259-1270
[27] Jwo, C. S., *et al*., Effects of Nanolubricant on Performance of Hydrocarbon Refrigerant System, *Journal of Vacuum Science and Technology B, 27* (2009), 3, pp. 1473-1477
[28] Vajjha, R. S., Das, D. K., Experimental Determination of Thermal Conductivity of Three Nanofluids and Development of New Correlations, *International Journal of Heat and Mass Transfer, 52* (2009), 21-22, pp. 4675-4682
[29] Incropera, F. P., *et al*., *Foundations of Heat Transfer*, 6th ed., John Wiley and Sons Inc., Singapore, 2013, pp. 897-924
[30] Cengel, Y. A., Ghajar, A. J., *Heat and Mass Transfer Fundamentals and Applications*, 4th ed., McGraw-Hill, New York, USA, 2011

[31] Patankar, S. V., *Numerical Heat Transfer and Fluid Flow*, Hemisphere Publishing Corporation, New York, USA, 1980, pp. 126-131
[32] Arslan, K., Three Dimensional Numerical Investigation of Turbulent Flow and Heat Transfer inside a Horizontal Semi-Circular Cross-Sectioned Duct, *Thermal Science, 18* (2014), 4, pp. 1145-1158
[33] Sieder, E. N., Tate, G. E., Heat Transfer and Pressure Drop of Liquid in Tubes, *Industrial Engineering Chemistry, 28* (1936), 12, pp. 1429-1435

Paper submitted: April 25, 2014
Paper revised: August 19, 2014
Paper accepted: November 28, 2014

© 2017 Society of Thermal Engineers of Serbia
Published by the Vinča Institute of Nuclear Sciences, Belgrade, Serbia.
This is an open access article distributed under the CC BY-NC-ND 4.0 terms and conditions